Elastic Scattering of Protons by Li^6†

WILLIAM D. HARRISON AND A. BRUCE WHITEHEAD
California Institute of Technology, Pasadena, California
(Received 26 July 1963)

The differential cross section for the elastic scattering of protons by Li^6 is presented at energies from 2.4 to 12 MeV and laboratory angles from 33.8° to 160°. A resonance appears strongly at backward angles at incident proton energy of 5 MeV suggesting the existence of a level in Be^7 at approximately 10 MeV. The possibility of this level being a ^4P state in Be^7 is discussed.

INTRODUCTION

THE Be^7 nucleus is known to have excited states at energies of 0.432, 4.54, 6.6, and 7.18 MeV.[1] In addition, the existence of a level has been suggested at an excitation of 14.6 MeV but remains unconfirmed. Thus, comparatively little is known about the region of excitation above 7.18 MeV. In the mirror nucleus, Li^7, there is evidence for the existence of six levels in this region although none has been confirmed.[1]

The ground and first excited states of Be^7 have spins and parities of $\frac{3}{2}^-$ and $\frac{1}{2}^-$, respectively[1] and are identified in the L-S coupling scheme as a doublet with $L=1$, $S=\frac{1}{2}$, commonly denoted ^2P. The level at 4.54 MeV with spin and parity of $\frac{7}{2}^-$ is then the lower member of the ^2F pair of levels. For some time the $\frac{5}{2}^-$ member of this doublet was missing until it was shown[2] that the 6.6-MeV level could be given this assignment. The similarity between the partial reduced widths of the 4.54- and 6.6-MeV levels helped to confirm the assignment in spite of a somewhat larger energy splitting than was predicted.[3]

The 7.18-MeV level was studied recently by McCray.[4] He was able to fit the angular distributions of protons elastically scattered by Li^6 assuming that the level was $\frac{5}{2}^-$ but he was unable to eliminate the possibility of a $\frac{3}{2}^-$ assignment. In his analysis, McCray assumed that the scattering could be described by the single resonant p wave plus a complex s-wave contribution on which he placed no restrictions. He did not include nonresonant scattering of p waves or higher waves. A tentative conclusion of his analysis was that one of the two s-wave phase shifts was going through resonance at an incident proton energy of 2.8 MeV, indicating the presence of a $\frac{1}{2}^+$ level at roughly 8-MeV excitation in Be^7. He pointed out, however, that this resonant behavior of the s-wave scattering might not be obtained under different assumptions about the mechanism of the p-wave scattering.

The $Li^6(p,\alpha)He^3$ reaction has been studied by Marion[5] and by Heydenburg[6] up to an energy in Be^7 of 15.5 MeV. Heydenburg obtained a yield curve at an angle of 70° which did not show any anomalies that might indicate the presence of new levels. His distributions, taken at 500-keV intervals, varied slowly with energy.

The $He^3(He^4,p)Li^6$ reaction has been studied by Tombrello and Parker.[2] Using the ONR-CIT tandem accelerator with the neutral helium injector, they were able to reach 8.4-MeV excitation in Be^7, covering the 7.18-MeV level. They observed the resonant yield of protons from this level but did not see a resonant contribution to the elastic scattering. Therefore, they supported McCray's conclusions that the level has a large reduced width for proton emission and a small reduced width for alpha emission. It is hoped with higher energies of He^3 particles, as for instance using the small current available from the negative ion injector, that this reaction may be used to reach considerably higher energies in Be^7.

No work has been reported on the inelastic scattering of protons from Li^6 although the proton group resulting from excitation of the 2.184-MeV level in Li^6 is readily observed. The spin restrictions associated with production of this 3^+ level open interesting possibilities for analysis. A study of this inelastic scattering is under way in this laboratory.

From shell-model predictions[3] a number of levels may be expected in the region of excitation from 7.2 to 15 MeV. If the 7.18-MeV level is the $^4P_{5/2}$ state, then there should be two more ^4P levels, namely $^4P_{3/2}$ and $^4P_{1/2}$. These should have partial reduced widths similar to those of the 7.18-MeV level. Also expected in this region are the lower lying nonnormal parity states beginning with $\frac{1}{2}^+$.[7]

In view of the large expected proton widths, it was felt that the $Li^6(p,p)Li^6$ elastic scattering process would be the simplest way to look for the other ^4P levels. In a preliminary account of the present experiment based on excitation yields at three angles[8] an anomaly was reported between 9 and 10 MeV in Be^7. Angular distributions have now been completed over the region.

† Supported by the U. S. Office of Naval Research.

[1] F. Ajzenberg-Selove and T. Lauritsen, Nucl. Phys. **11**, 1 (1959).
[2] T. A. Tombrello and P. D. Parker, Phys. Rev. **130**, 1112 (1963).
[3] D. R. Inglis, Rev. Mod. Phys. **25**, 390 (1953).
[4] J. A. McCray, Ph.D. thesis, California Institute of Technology, 1962 (unpublished); Phys. Rev. **130**, 2034 (1963).
[5] J. B. Marion, G. Weber, and F. S. Mozer, Phys. Rev. **104**, 1402 (1956).
[6] N. P. Heydenburg and I. G. Han, Bull. Am. Phys. Soc. **7**, 58 (1962) and (private communication).
[7] A. M. Lane, Rev. Mod. Phys. **32**, 519 (1960).
[8] W. D. Harrison and A. B. Whitehead, Bull. Am. Phys. Soc. **6**, 505 (1961).

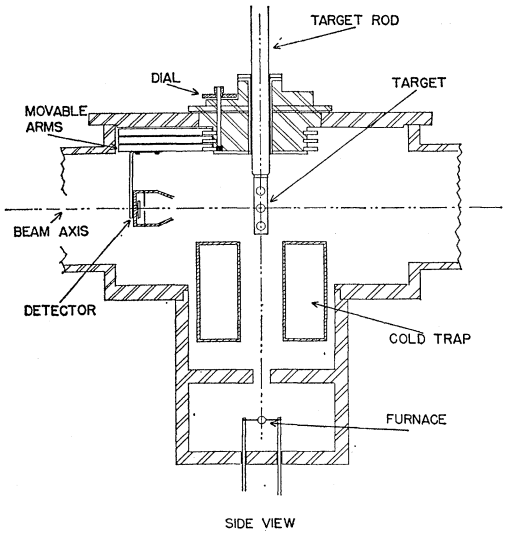

FIG. 1. Side view of scattering chamber with the central foil of the target holder positioned on the beam axis. All three movable arms are shown but only one detector, located in the 180° position, and one dial and pinion are included. The locations of the toroidal cold trap and furnace chamber are illustrated.

APPARATUS

The proton beam from the ONR-CIT tandem accelerator was directed into the scattering chamber shown in Fig. 1. The energy range from 2.4 to 12 MeV was covered in the course of the experiment. Targets were made by evaporating separated Li^6 (isotopic abundance 99%) onto a thin carbon foil or, in later experiments, a thin nickel foil. The carbon foil tended to extend and wrinkle during the evaporation. The area being irradiated by the proton beam then tended to contract, producing a gradually thickening target. Most of the angular distributions were taken using targets with the carbon foil backings and the target thickness was carefully monitored with a fixed angle detector. The nickel backing was subsequently found to be more reliable and was used for all of the excitation functions.

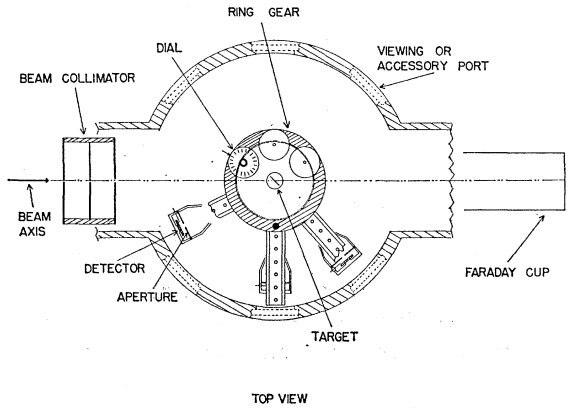

FIG. 2. Top view of scattering chamber. The beam entrance port is shown with collimator in place. The Faraday cup is indicated schematically. Three detectors are shown mounted on movable arms. The inside diameter of the chamber is 25.4 cm.

Evaporation took place in a separate vacuum system accessible through the bottom of the target chamber. When the target holder was extended down into the furnace chamber, the target rod sealed the opening to the scattering chamber. A "cannon-shaped" furnace was constructed using 0.0025-cm tantalum foil. The thickness of the Li^6 on the various targets used in the course of this experiment ranged from 30 to 300 $\mu g/cm^2$.

The spectrum of particles emitted from the target was detected with lithium-drifted solid-state detectors[9] or surface-barrier detectors[10] constructed in this laboratory. The advantage of lithium compensation over the surface-barrier effect is that the former produces a much deeper depletion layer in the crystal and therefore responds to much more penetrating particles. Protons with energies up to 12 MeV produced pulses from the detector which were strictly proportional to their energy. The resolution was typically 200 keV for the lithium-drifted detector and better than 100 keV for the surface barrier. At some energies and angles aluminum foil was used over the detector to separate the proton group from the He^3 and He^4 groups.

The chamber was designed so that three independently movable detectors could be used simultaneously (Figs. 1 and 2). Each detector was mounted on an arm which was, in turn, secured to one of the three stacked ring gears. Each ring gear was driven by a small pinion wheel located to mesh with the teeth on the inner radius of the gear. The gear ratio was 18:1 and the face of the dial which was mounted on the pinion axis was inscribed with 20 equally spaced divisions. Thus, a rotation of one dial division produced a detector rotation of 1° about the target. Each detector viewed a solid angle determined by a limiting aperture 0.32 cm in diameter located 10 cm from the target.

Six accessory ports were located around the side of the chamber at 45° intervals. They could be used either for viewing, for inserting a small quartz disk into the center of the chamber, or for mounting additional detectors.

Pulses from each detector were fed to a Tennelec preamplifier and subsequently to a Hamner nonoverloading amplifier. The single-channel discriminator on the Hamner amplifier was set to include the portion of the pulse spectrum containing the elastic proton group, and counted with a conventional scaler.

An RIDL multichannel pulse-height analyzer was used in estimating the background or continuum portion of the spectrum to be subtracted from the scaler counts.

During the course of this experiment it was found that the use of three detectors simultaneously presented normalizing and data handling problems so only one detector was used for most of the accurate work.

[9] Y. R. Cusson and M. E. Nordberg (private communication).
[10] G. Dearnaley and A. B. Whitehead, Nucl. Instr. Methods 12, 205 (1961).

RESULTS

Preliminary yield curves were taken at laboratory angles of 86.4°, 120°, and 152.5°. The incident proton energy was varied from 2.4 to 11 MeV in approximately 50-keV steps. The interesting feature present in the yield curves was a broad peak near an incident proton energy of 5 MeV which was more pronounced at the backward angle than at 86.4°. The energy range between 3 and 5 MeV was scanned with increments of 20 keV to minimize the possibility of a narrow resonance existing unobserved in that region. The conclusion that only one broad anomaly existed in Be^7 between 7.5 and 15-MeV excitation was reported at the American Physical Society meeting in December 1961.[8]

Consequently, energy steps of 200 keV were chosen for mapping of the yield as a function of energy and angle. Above 6 MeV, angular distributions were taken in 1-MeV intervals.

A complete set of data is given in Table I. The angular distribution at each energy was obtained using one movable detector and a monitor at a fixed angle. Thus, any changes in target thickness during the run were corrected. Excitation functions were taken at the two lab angles 80.5° and 160°, each with a target whose thickness was rechecked repeatedly at a fixed energy and was found not to fluctuate. As a check, many points distributed throughout the angle and energy range were remeasured using a particularly uniform target. Additional data were taken using this target and proton energies in half-MeV increments from 6 to 12 MeV at lab angles of 80.5° and 116.7°. The stated accuracy given for each point in Table I was estimated from the statistics of the measurement, the magnitude of background which had to be subtracted, and the accuracy with which data from that particular target could be normalized.

Finally, the entire set of self-consistent data was normalized to the differential cross sections obtained by McCray[4] in the region of incident proton energy from 2.4 to 2.8 MeV.

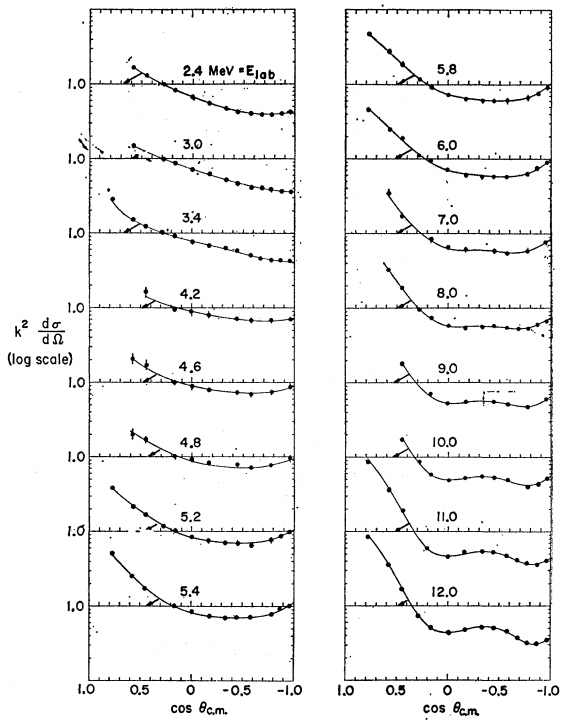

FIG. 3. A selection of angular distributions for $Li^6(p,p)Li^6$. Smooth curves are drawn through all data points.

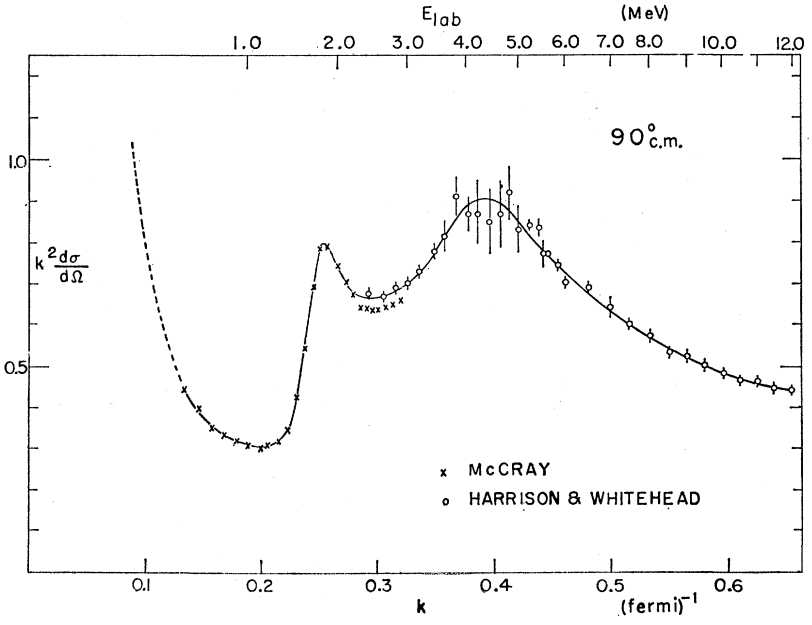

FIG. 4. Excitation function at 90° center of momentum.

TABLE I. Differential cross section for $Li^6(p,p)Li^6$ in mb/sr; E_{lab} is the incident proton energy in MeV; θ_{lab} is the laboratory scattering angle; $\theta_{c.m.}$ is the scattering angle in the center-of-momentum system. Probable errors are given.

θ_{lab} (deg)	$\theta_{c.m.}$ (deg)	$\cos\theta_{c.m.}$	$E_{lab}=2.4$ $d\sigma/d\Omega$	Error (%)	$E_{lab}=2.6$ $d\sigma/d\Omega$	Error (%)	$E_{lab}=2.8$ $d\sigma/d\Omega$	Error (%)	$E_{lab}=3.0$ $d\sigma/d\Omega$	Error (%)	$E_{lab}=3.2$ $d\sigma/d\Omega$	Error (%)	$E_{lab}=3.4$ $d\sigma/d\Omega$	Error (%)	$E_{lab}=3.6$ $d\sigma/d\Omega$	Error (%)	$E_{lab}=3.8$ $d\sigma/d\Omega$	Error (%)
33.8	39.1	0.775									243	3	230	3				
47.6	54.8	0.576	198	2	169	2			141	3	129	1	122.8	1				
55.5	63.4	0.449	153	1	133	2	121	2			105.5	1	101.5	1	102	15	97	15
65.0	73.7	0.281	117	1	103.0	1	96.5	2	91.0	1	86.9	1	83.8	2				
71.3	80.4	0.167	96.8	2	88.7	1	84.0	2	81.0	1	77	6	74.8	2	72	5	72	5
80.5	90.0	0.000	79.2	2	72.2	2	69.5	2	66.0	2	64.2	2	64.7	3	63	5	67	5
90.0	99.6	−0.167	65.0	2	60.0	3	58.0	3	58.4	2	58	7	56.7	3	58	7	58.1	2
100.0	109.4	−0.331	55.3	2	49.6	4			48.0	3	48.1	5	52.0	3			52.3	2
107.4	116.5	−0.446	49.7	2	45.0	4	44.5	3	43.0	5	43	10	47.7	2	44	7	48.3	2
116.7	125.3	−0.578	47.2	5	41.3	5	38.8	4	38.9	5	39	10	41.6	2	40	7	42	7
125.0	132.7	−0.678	46.2	5	38.8	5	36.8	4	38.0	2	37.4	2	37.8	2			43.3	2
133.8	140.7	−0.774	46.0	5	38.2	5	37.1	3	35.1	5	34.1	3	37.0	3	37	5	42	5
145.0	150.5	−0.870	47.1	5	38.8	5	35.5	3	34.1	2	33.8	2	35.6	3			41.1	2
160.0	163.3	−0.958	48.4	5	40.8	4	35.2	4	33.3	3	33.4	2	34.9	2	37	6	42	6

θ_{lab} (deg)	$\theta_{c.m.}$ (deg)	$\cos\theta_{c.m.}$	$E_{lab}=4.0$ $d\sigma/d\Omega$	Error (%)	$E_{lab}=4.2$ $d\sigma/d\Omega$	Error (%)	$E_{lab}=4.4$ $d\sigma/d\Omega$	Error (%)	$E_{lab}=4.6$ $d\sigma/d\Omega$	Error (%)	$E_{lab}=4.8$ $d\sigma/d\Omega$	Error (%)	$E_{lab}=5.0$ $d\sigma/d\Omega$	Error (%)	$E_{lab}=5.2$ $d\sigma/d\Omega$	Error (%)	$E_{lab}=5.4$ $d\sigma/d\Omega$	Error (%)
33.8	39.1	0.775													211	3	263	5
47.6	54.8	0.576							127	15	119	15	121	15	118.0	2	132	3
55.5	63.4	0.449	99	5	108	15	118	15	105	15	100	7	100	7	90.8	2	89.0	3
65.0	73.7	0.281													63.6	2		
71.3	80.4	0.167	70	5	64	6	63	5	61	7	58	7	61	7	56.8	5	52.7	3
80.5	90.0	0.000	61	5	58	10	54	10	53	10	54	7	47	7	45.4	1	43.2	3
90.0	99.6	−0.167	58	5	55	10	52	10	49	6	49	6	46	6	39.5	6	38.5	3
100.0	109.4	−0.331													38.9	2	36	5
107.4	116.5	−0.446	50	5	48	6	45	6	45	6	46	5	41.5	5	38	8	37.0	3
116.7	125.3	−0.578	48	5	45	7	45	7	42	7	42	5	41.1	5	35	7	37.5	3
125.0	132.7	−0.678																
133.8	140.7	−0.774	45	5	45	6	47	7	45	7	45	5	43.4	5	42	8	41.0	3
145.0	150.5	−0.870													47.6	1	48.0	3
160.0	163.3	−0.958	45	5	48	6	50	7	54	10	56	5	55.0	5	52.8	2	54	4

TABLE I (*continued*).

θ_{lab} (deg)	$\theta_{c.m.}$ (deg)	$\cos\theta_{c.m.}$	$E_{lab}=5.5$ $d\sigma/d\Omega$	Error (%)	$E_{lab}=5.6$ $d\sigma/d\Omega$	Error (%)	$E_{lab}=5.8$ $d\sigma/d\Omega$	Error (%)	$E_{lab}=6.0$ $d\sigma/d\Omega$	Error (%)	$E_{lab}=6.5$ $d\sigma/d\Omega$	Error (%)	$E_{lab}=7.0$ $d\sigma/d\Omega$	Error (%)	$E_{lab}=7.5$ $d\sigma/d\Omega$	Error (%)	$E_{lab}=8.0$ $d\sigma/d\Omega$	Error (%)
33.8	39.1	0.775					229	3	222	3							237	3
47.6	54.8	0.576			133	8	135	8	119.7	1			143	10			116	3
55.5	63.4	0.449			95	8	91	8	90	5			71	10			64.3	3
65.0	73.7	0.281					56.6	1	51.4	1							34.4	3
71.3	80.4	0.167			49	7	46.5	5	44.5	5			33	7			25.3	3
80.5	90.0	0.000	39.5	3	38.5	5	35.9	2	33.0	1	29.9	2	25.6	5	22.5	3	20.1	3
90.0	99.6	−0.167			36	7	30.9	2	28.5	5			24	7			19.5	3
100.0	109.4	−0.331					29.0	5	27.0	5							20.2	2
107.4	116.5	−0.446			34	6	29.5	6	27.0	5			23	7			19.9	2
116.7	125.3	−0.578	32.5	3	33	6	30	10	26.9	2	24.0	4	22.0	3	19.9	2	19.0	2
125.0	132.7	−0.678															18.8	2
133.8	140.7	−0.774			36	7	32	12	29.5	5			24	7			18.7	2
145.0	150.5	−0.870					37.3	2	34.5	5							21.0	2
160.0	163.3	−0.958			48	8	44	8	42.0	5			30	7			23.9	3

θ_{lab} (deg)	$\theta_{c.m.}$ (deg)	$\cos\theta_{c.m.}$	$E_{lab}=8.5$ $d\sigma/d\Omega$	Error (%)	$E_{lab}=9.0$ $d\sigma/d\Omega$	Error (%)	$E_{lab}=9.5$ $d\sigma/d\Omega$	Error (%)	$E_{lab}=10.0$ $d\sigma/d\Omega$	Error (%)	$E_{lab}=10.5$ $d\sigma/d\Omega$	Error (%)	$E_{lab}=11.0$ $d\sigma/d\Omega$	Error (%)	$E_{lab}=11.5$ $d\sigma/d\Omega$	Error (%)	$E_{lab}=12.0$ $d\sigma/d\Omega$	Error (%)
33.8	39.1	0.775											228	3			204	3
47.6	54.8	0.576											97.2	3			82.6	3
55.5	63.4	0.449			56.5	5			47.8	5			48.3	3			40.3	3
65.0	73.7	0.281							23.6	4							17.3	3
71.3	80.4	0.167			22.0	5			16.3	4			15.3[a]	3[a]			11.5	3
80.5	90.0	0.000	17.7	3	16.4	3	15.0	3	13.5	3	12.5	3	11.8	3	10.9	3	10.3	3
90.0	99.6	−0.167			17.0	2			14.6	3			13.4	3			11.2	3
100.0	109.4	−0.331							15.2	4			13.8	3			12.4	3
107.4	116.5	−0.446			17.3	2			15.0	3			13.4	3			11.8	3
116.7	125.3	−0.578	17.3	2	16.2	2	15.0	2	13.6	3	12.6	3	12.0	2	11.15	2	10.6	2
125.0	132.7	−0.678											10.3	3			8.62	3
133.8	140.7	−0.774			14.7	2			11.2	3			9.83	3			7.45	3
145.0	150.5	−0.870							12.5	4			9.19	3			7.17	3
160.0	163.3	−0.958			18.7	2			14.5	3			10.4	3			7.98	3

[a] At $\theta_{lab}=69°$.

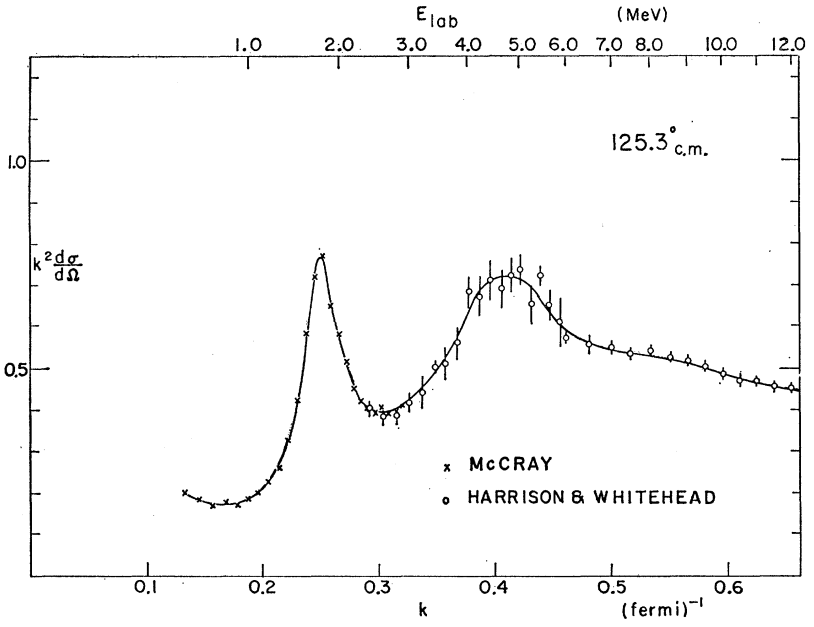

FIG. 5. Excitation function at 125.3° center of momentum.

McCray states an absolute probable error of $\pm 5\%$ for the normalization of the differential cross sections which he obtained. McCray's excitation functions were interpolated to give differential cross sections at the energies for which we obtained angular distributions. Smooth angular distribution curves were drawn through the present data at these energies and the 18 points derived from McCray's data were compared with the curves. The correct normalizing factor for the present data was determined in this way with an accuracy of $\pm 1\%$. McCray's data point at 90° center-of-momentum fell consistently below the smooth curve drawn through the present data, although agreement at other angles was good.

Angular distributions were plotted at each energy using the dimensionless quantity $k^2 d\sigma/d\Omega$ as abscissa and $\cos\theta_{\text{c.m.}}$ as the ordinate. k is the wave number of the bombarding protons, $d\sigma/d\Omega$ is the differential scattering cross section and $\theta_{\text{c.m.}}$ is the scattering angle. All quantities are expressed in the center-of-momentum system. A selection of these distributions is given in Fig. 3. Excitation functions at the center of momentum angles 90°, 125.3°, and 180° (extrapolated) were plotted using $k^2 d\sigma/d\Omega$ as abscissa and k as ordinate. These are shown in Figs. 4–6 together with data points by McCray. An incident proton energy scale, E_{lab}, is given.

DISCUSSION

A rigorous analysis of the data was not performed. The straightforward procedure is to fit the partial-wave expansion for the cross section to the observed data, extracting a coefficient for each angular dependent term. In simple cases, these coefficients determine the phase shifts and, hence, parameters of any resonances. In other cases, when particles have spin and reaction channels are open, these coefficients do not completely determine the phase shifts, and further information about reaction channels or polarization is needed. This is the situation that applies to the present experiment.

If several l values contribute to the scattering, this kind of analysis requires data of extremely high accuracy over the entire range of angles. (For s and p waves there are seven coefficients to be determined.) Several l values are expected to contribute at the energies involved in the present experiment, making a rigorous analysis of data of the accuracy attained unfeasible.

An alternative approach is to make physically reasonable guesses for resonant and nonresonant phase shifts. These are used to generate the cross section which is then compared with experiment. This procedure may suggest which parameters are most likely to be resonant. The difficulty with $Li^6(p,p)Li^6$ in the energy range of this experiment is the large number of parameters. For s waves alone there are 2 complex phase shifts, for s and p waves there are 9. Preliminary work carried out along these lines was inconclusive.

Nevertheless, qualitative information may be obtained from the data. From the excitation functions, Figs. 4–6, a peak is observed at $E_{\text{lab}}=5$ MeV. It is most prominent at 180° and smallest at 90°, a behavior which is similar to that of the peak at $E_{\text{lab}}=1.8$ MeV. It can probably be attributed to a single resonance in the compound nucleus, Be^7, at about 10 MeV. The data also suggest a slight feature at 8- or 9-MeV bombarding energy which may be evidence for further structure in Be^7.

A crude estimate of the width of the 10-MeV level may be made from the 180° excitation curve. The

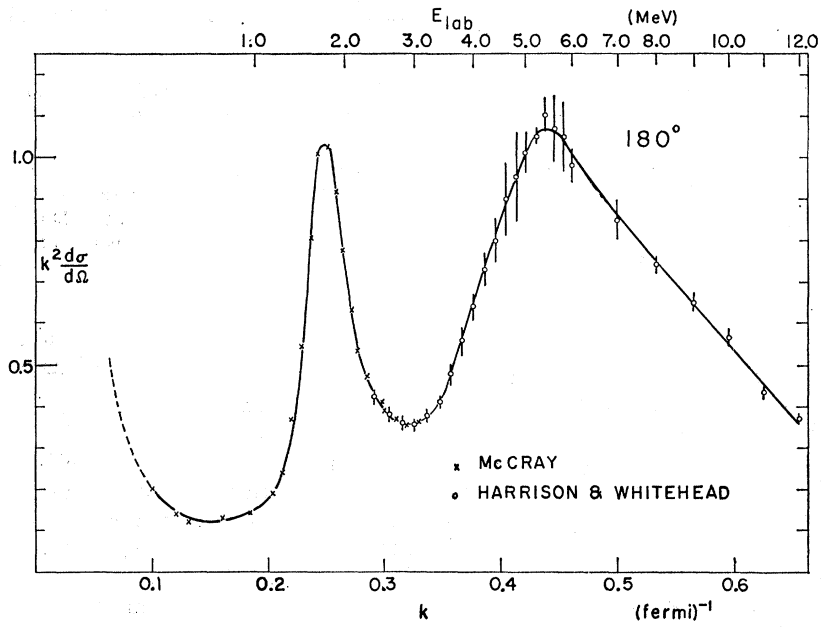

FIG. 6. Excitation function at 180°. The points are extrapolated from the data.

similarity between the 5-MeV resonance and the 1.8-MeV resonance suggests that both are produced by the same partial wave, p-wave protons. On this assumption, one obtains a reduced width for proton emission of the order of 3 ± 2 MeV-F for the upper resonance, to be compared with McCray's value of 5 MeV-F for the lower level.

The similarity between the two levels can be further brought out by examining the $Li^6(p,\alpha)He^3$ data of Heydenburg[6] in the region of 5-MeV bombarding energy. There is no apparent rise in the α yield in this region, implying that if a level exists, it has a small width for α emission. For the lower level, McCray obtained a reduced α width of 0.1 MeV-F, more than an order of magnitude smaller than the reduced proton width. It might be pointed out that the most logical shell-model assignment[3] for the 7.18-MeV level and perhaps for the 10-MeV level is ^4P. In this configuration the three outer nucleons have a total orbital angular momentum $L=1$ and total spin $S=\frac{3}{2}$, requiring a spin change of one unit before the levels could decay to He^4+He^3. Thus, ^4P levels are expected to exhibit small reduced widths for decay into this channel.

The cross sections for the many-body breakup reactions,

$$Li^6+p \rightarrow He^4+p+d, \text{ threshold } E_{lab}=1.72 \text{ MeV}$$
$$\rightarrow He^4+2p+n, \text{ threshold } E_{lab}=4.30 \text{ MeV}$$

are not known, but a large continuum in the spectra taken indicates that these may be large.

CONCLUSIONS

The data suggest strongly the existence of a level in Be^7 at 10 MeV. The similarity in behavior between this level and the lower level at 7.18 MeV suggests that they are members of the same multiplet, ^4P in L-S coupling notation according to the shell model. Although the predicted order of the members of this quartet is $^4P_{5/2}$, $^4P_{3/2}$, $^4P_{1/2}$, it is not evident from this experiment which J value should be assigned to the 10-MeV level.

ACKNOWLEDGMENTS

The authors wish to thank the members of the Kellogg Radiation Laboratory, particularly Professor T. Lauritsen and Professor C. A. Barnes for many helpful discussions and encouragement. We would also like to thank Dr. J. A. McCray and Dr. N. Heydenburg for access to their data before publication.